AADE-08-DF-HO-04

Geomechanics Modeling for Better Drilling Performance

Hong (Max) Wang, Mohamed Y. Soliman, Zhaohui Shan, Halliburton; Brian F. Towler, University of Wyoming

Abstract

Geomechanics modeling is very important for optimizing drilling performance by increasing rate of penetration (ROP) and minimizing non-productive time (NPT). It provides the basis for bit selection and drilling parameter optimization, wellbore stability analysis, and lost circulation prevention and control. Because of difficulties accessing the rock formation, the modeling largely relies on the data availability and quality. To narrow down the error bar during the process, a vast amount of data may be needed for cross-checking the modeling quality.

Using a real case from a cuttings injection project, it is demonstrated what data are needed, which documents contain the data and how the raw data are processed to obtain the needed parameters for further engineering simulation.

Introduction

Rotary drilling has long been the major means to access hydrocarbon reserves. During the drilling process and the penetration of subterranean rock formations, rock will be constantly exposed to alterations due to mechanical and chemical interactions. Attempts to improve drilling efficiency without integrating geomechanics will not reach the optimum.

However, due to the difficulty of accessing the rock in-situ, the cost of knowing the rock properties is generally very high. Gaining knowledge of the rock requires acquisition of a batch of data and processing the data for rock properties. Further, simulations are needed to understand the rock behavior under certain drilling conditions.

With the development of computer technologies, the data acquisition and processing cost has gone down and the value created out of understanding the rock behavior has gone up. Especially as rig costs increase, the value of understanding rock is tremendous. This trend has created opportunities for operation optimization and drilling process innovation as well.

The major role of geomechanics in drilling currently includes the following:

- Drilling method selection (underbalanced/managed pressure drilling, conventional drilling, casing drilling, etc.)
- Well design for optimized well trajectories and casing programs;
- Drill bit customization and selection for improved ROP and borehole quality;
- Drilling parameters optimization for high ROP;
- Wellbore stability indicators for drilling fluid selection and optimization;
- Wellbore strengthening for higher wellbore pressure containment and coping with lost circulation.

Well design starts with understanding the subterranean stress and pressure profiles and lithologies. Selecting the best method of drilling can significantly reduce well construction costs, as demonstrated by a progressive reduction in total drilling days in a new drilling area. The number of drilling days required can be greatly shortened after a number of wells have been drilled and performance has been analyzed for better well designs.

Better designs also include optimized casing points and well trajectories including wellbore deviation and azimuth with an understanding of the effects of stress, strength and pressure environments.

Drill bit design, selection and usage should all be tied to the understanding of geomechanics[1] including the lithology, rock strength, shale plasticity, formation pressure, abrasiveness, etc. Bit selection software programs have been created to allow engineers to select the best bit for an interval based on the geomechanical properties of the formations to penetrate. Understanding rock properties is also necessary to help ensure the bit achieves the optimal ROP and to diagnose improper usage of a drill bit.

Wellbore stability analysis has long been performed for obtaining a minimum mud weight for critical drilling projects. In addition to the mud weight, understanding of the hole collapse mechanisms is equally important for correct mud chemistry, such as selecting the right mud type, preparing an optimized water phase salinity, etc.[2,3] The stress and pressure environment, as well as the rock strength, also play important roles. Because wellbore stability is strongly related to the wellbore orientation, the proposed wellbore deviation and azimuth are needed as well. Rock sensitivity to water and various cations, shale water activities, CEC (Cation Exchange Capacity), etc. together with rock mechanical properties are all necessary to depict the rock behavior under wellbore stability conditions.

Wellbore strengthening is a new concept[4,5,6] that has led to a series of studies[7,8,9,10] and subsequent field successes.[11,12,13] Wellbore strengthening techniques can help operators achieve higher wellbore pressure containment and contribute to studies to understand why some wellbores are weaker than others.[8] Similar to wellbore stability analysis, designing a wellbore strengthening job (sometimes referred to as stress cage) requires knowing almost the same types of data as wellbore stability analysis. Knowing the rock parameters, etc. allows us to perform simulations to understand fracture dimensions and determine the best treating materials and engineering design.

Geomechanics can be also important to Health, Safety and Environment (HSE) considerations. One of the important examples is cuttings injection design. It requires substantial understanding of a geomechanical environment before a good injection simulation can be performed with a computer software program. Only with the integration of the geomechanics and injection simulation, can a safe disposal domain be designed. Even during the injection process, geomechanical understanding is necessary to explain pressure anomalies and allow us to make smart operational decisions.

Aside from drilling, geomechanics can be extended to completion and production optimization for sand control, stimulation, etc. In a word, geomechanics has been playing an increasingly important role in drilling and other petroleum engineering aspects as well.

Data Requirements

For different drilling applications, different sets of geomechancs parameters may be needed. However, in general they fall into the following categories:

- Wellbore geometry
- Rock mechanical properties
- Stress and pressure
- Wellbore fluids
- Fluid and rock interaction

Wellbore geometry accounts for the hole size, deviation, azimuth, length of an openhole interval, etc.

Rock mechanical properties may at least include Young's modulus and Poisson's ratio. Rock strength, permeability, and other properties may also be needed depending on the interest of investigation.

Stress magnitudes and orientation are very important for the wellbore stability that is a key design criterion for drilling. Formation pressure and fracture gradients define an initial mud weight window. Furthermore, wellbore stability should be considered for this window. If this window is not wide enough, wellbore strengthening may be applied to widen the mud weight window.

Wellbore fluids provide information about the chemistry, rheology and particulate type and concentration. These are all important for understanding wellbore behaviors. Rig daily operations provide information about fluid and rock interaction. This can also be obtained through pressure tests such as leak-off tests (LOT).

Data Collection

These data are generally obtained through analysis of the following documentations:

- Well diagrams
- Formation Pressure, Mud weight, Frac Gradient Profile Plots
- Drilling, Mud and Mud Logging reports
- Logs
  - Full Wave Sonic (Compressional & Shear)/other sonic logs
  - Density/Neutron/GR/Caliper/Borehole image logs
  - Formation pressure tests
  - Other logs
- Region information
  - Basin study report/Seismic map/Fault map
- Other information
  - Core test report, cuttings analysis report
  - Well testing, hydraulic fracturing report or water injection report
  - LOT/Extended LOT

Due to the wide range of data source, such analysis normally requires extended knowledge and experience in order to extract the valuable information out of the documentations.

Data Analysis

Rock mechanical properties can be obtained through lab tests. However, rock samples are normally not readily available because coring, sample preservation, HTHP testing, etc. can be complicated and costly procedures. A more common methodology is a so called log-based analysis. Results from lab tests can then be used as calibrations. **Table 1** summarizes methods for obtaining various parameters for drilling related geomechanics analysis. Data quality control is always a necessary step for generating correct results.

Case History

To demonstrate the data analysis process, here we include an actual case history for cuttings injection simulation. This simulation was done for performance analysis of a cuttings injection project that has been going on for several years. Due to confidentiality, critical information has been removed for this publication.

A geomechanical model must be constructed to provide a base structure for cuttings injection simulations. It is critical that the model reflect the best understood reality as closely as is practical, so that the simulated operational parameters result in output that represents real world performance. This is necessary in order to ensure the safe and efficient disposal of the drilling wastes.

Geomechanical modeling incorporates pore pressure and effective stress values in developing an understanding of the total active stresses. It is critical to understand the permeability, Young's modulus, etc. in order clarify total active stresses. Due to the fact that limited direct data are normally available for potential cuttings injection disposal zones, more expertise is required to understand and describe the geomechanical environment for these operations than for typical hydraulic fracturing design.

In hydraulic fracturing, pore pressure is normally known with well testing methods or production records. However, for cuttings injection it is quite likely that pressure and stresses will have to be determined simultaneously by solving the related correlation equations using the limited known data points for total stresses at given depths.

Stress Environment: The Big Picture

One of the first tasks in developing the geomechanical model was determination of the stress environment in the disposal zone. The pertinent acquired log data were reviewed for quality control as a first step in the process. No log quality issues were identified.

Stepping further back in reviewing the stress in the area, the stress environment was better understood in light of plate tectonics in the area. It was found that the area of interest is in a unique strike/slip environment. Due to colliding movement of the two continental plates, severe stress anisotropy should be expected. The world stress map indicates strike-slip and thrust faulting regimes with the strike in the nearly N-W direction. The compression stress component, therefore, is maximized in the NW direction.

This understanding is essential for selecting a good approach to determine the stress environment. Details and figures are omitted here to protect the confidential information.

Determining the Lithology

The lithology was determined utilizing the provided logs. During a log-based analysis, differentiation was achieved primarily with the gamma ray log and translated into shale volumes by making use of the mud logs, as well as the other logs provided. The formations of interests were determined to be claystone and sandstone.

Determining the Closure Pressure

The closure pressure was analyzed with the SQRT Time Plot, G-Function Plot, GdP/dG Plot. This is demonstrated with the LOT #1 data. **Figure 1** represents the plots of LOT #1 and LOT #2. **Figure 2** is the analysis plot with the SQRT method. **Figure 3** is the analysis plot with the G-Function method. **Figure 4** is the analysis plot with the Gdp/dG method.

Table 2 summarizes the pressure decline analysis (PDA) for the LOT #1 on closure pressure at the depth of 7907 ft (2410 m) with the three methods.

These results are very close to one another with an average of 15.9 ppg, which is the same as determined directly from the LOT raw data plot. Many times, these results don't agree with each other and one has to be cautious to select the correct result.

With the same method, some other pressure decline data from cuttings slurry injection were analyzed and the summary of some the data are listed in **Table 3**.

In **Table 3**, there are two data sets with significant variance from the others. The first one is the determination of a 15.87 ppg equivalency from LOT#1. This is a significantly lower value than the average. It is possibly due to the strong stress anisotropy which creates a low tangential stress area at and near the wellbore. This effect would not be seen again after the fracture has grown into the far field area. Apparently in this case, the fracture initiation pressure is smaller than the far field minimum horizontal stress.

The second notable variance is the 18.98 ppg result for Injection#2. This might have been caused by solids accumulation inside the fracture that might possibly increase the stress at closure. Cleaning the solid deposit or creating a new fracture would reduce the closure pressure back to what is close to the far field stress – minimum horizontal stress. Subsequent batches showed reduced pressures and the variance that has occurred during the life of the injection project point to some significant transient dynamics of solids placement and movement in the disposal zone.

After eliminating the two data sets in question, an average of 0.94 psi/ft or 18.12 ppg equivalent minimum horizontal stress was determined for the depths of injection.

Determining Permeability

Determination of the permeability from the available data remains approximate. Leak-off tests were first performed on the originally targeted claystone formation at the base of the injection zone. Due to the limited nature of the pressure decline data available, a pressure decline analysis method developed by Soliman[14] was applied to the test data to determine the permeability. This method can also be used to obtain a formation pressure estimate. It requires identification of the flow regime with a $-tdP/dt$ versus t plot, from which a constant for calculating permeability can be defined with $(P_i-P_w)t^n$ versus t. The pore pressure can also be determined at the same time. A summary of this technique is given in appendix.

Figure 5 indicates the results from two LOT tests performed at 7907 ft with a brine fluid of 9.1 ppg. Utilizing Soliman's method, a claystone permeability of 0.14 md was determined from LOT #1, as shown in **Figure 6**. The bleed-back volume from the LOT #1 test was 1.2 bbl after 40 minutes of shut-in. A total of 6.5 barrels were injected at a rate of 0.3 bpm. This volume of fluid loss indicates a relative larger permeability than normally expected in claystone formations. This permeability should be the average of the matrix and natural fractures if they exist.

However, due to the short such-in time, the interpreted permeability can be higher than the reality. The interpreted value can be used as an upper bound for the claystone formation permeability for the cuttings injection simulation.

Neither the SP log, nor resistivity logs show good indications of permeability of any formations. It is believed that the sandstone formations may have relatively low permeability.

Determining the Pressure

The pressure decline analyses were performed on the test and injection data in order to better understand the nature of in situ pressure before and during the injection operations. Analysis was demonstrated with data acquired from LOT #1. The analysis plots are displayed in **Figure 7** and **Figure 8**. A summary of a selection of the test results can be found in the **Table 4**. These results were either obtained by the Horner or Soliman's methods. These analyses were performed to determine pressure in the claystone formations.

While the provided resistivity logs and density logs reveal no indication of significant abnormally pressured zones, analyses do indicate pressures consistently higher than a normal pressure gradient of 0.45 psi/ft. However, this is inconsistent with a review of the mud weights used in drilling the well to provide an estimate of pore pressure in the sandstone. (Refer to the Track "PS ppg" on the log analysis, **Figure 9**). The low mud weights used indicate a normal pressure gradient in the sandstone formation, which would tend to indicate higher permeability and formation extent, which would have allowed equilibration of pressure over geologic time. A typically very low permeability claystone might be expected to be sufficiently non-transmissive such that pressure would not be dissipated, however, the permeability of the claystone has been previously estimated to be approximately 0.14 md. With that permeability, the pressure gradients in the claystone and sandstone formations should be basically identical.

Based on the findings, it is believed that the pore pressure gradient is approximately normal and a 0.455 psi/ft pressure gradient was assumed in both sandstone and claystone formations at the depths of interests.

Analyses show a gradual increase in pressure with increasing injection time, indicating the additive effects of continued waste injection. Therefore, the early data best represents the far initial reservoir pressure. For a large body of the fluid injection, an increasingly longer shut-in time should be expected to obtain and estimate of the original formation pressure, especially when the formation permeability is relatively low.

Determining the Minimum Horizontal Stress

There are different methods for interpreting horizontal stresses. But, many of them have limitations and they all need calibration with some other data source, such as pressure tests. The method used herein is an "effective stress" method, which assumes that there is a correlation between the vertical stress and horizontal stress in shale. The method requires the knowledge of the overburden stress. The vertical stress was assumed to be 1.0 psi/ft, where the density log was not available for depths shallower than 1000 meters. The interpreted stresses are calibrated to the LOT results. Refer to Track "PS ppg" in Figure 9 for minimum horizontal stress designated as Shm_ppg.

Determining Young's Modulus and Poisson's Ratio

Young's Modulus and Poisson's Ratio were derived using a synthetic sonic log based on the following equations:

$$E = \frac{\rho v_s^2 \times \left[3\left(\frac{v_p}{v_s}\right)^2 - 4 \right]}{\left(\frac{v_p}{v_s}\right)^2 - 1}$$

and

$$\nu = \frac{\left(\frac{v_p}{v_s}\right)^2 - 2}{2\left[\left(\frac{v_p}{v_s}\right)^2 - 1\right]}$$

where,

ν_p – compressional velocity
ν_s – shear velocity
ρ - density from density log

Conversion to static values was performed by taking porosity into consideration. The analysis indicates that the Young's Modulus is about 1.5 and 2.0 million psi for claystone and sandstone respectively and Poisson's Ratio is about 0.3 for both claystone and sandstone. Refer to Track "Mechanical Properties" in Figure 9.

Simulation Results

With the geomechanical model created, a multiple batch simulation was performed to see whether the result will match with recorded data.

Figure 10 shows the result of a 7400 min multiple batch injection simulation. It is the bottomhole injection over time. The recorded data for the same period of time is displayed in **Figure 11**. It can be seen that they match very well. **Figure 12** shows the multiple fractures generated from the simulator for this 7400 min multiple batch injection period.

Conclusions and Summary

- Geomechanics modeling can provide the basis for improving drilling performance in various aspects.
- Data categories are summarized and data documentations are listed for data collection.
- Data analysis for geomechanics modeling requires a wide range of knowledge and experience in order to extract and integrate the data into the model.
- A general process was demonstrated with an actual case history for cuttings injection performance analysis.
- The case study indicates that the new method for pore pressure and permeability analysis was easy to use.

Acknowledgments

The authors would like to thank Halliburton for granting permission to publish the paper.

Nomenclature

CEC – Cation Exchange Capacity
ELOT – Extended Leak-Off Test
EMW – Equivalent Mud Weight
GR – Gamma Ray
HSE – Health Safety Environment
HTHP – High Temperature High Pressure
ISIP – Instantaneous Shut-In Pressure
LOT – Leak-Off Test
NPT – Non-Productive Time
PDA – Pressure Decline Analysis
ROP – Rate of Penetration
SP – Spontaneous Potential
SQRT – Square Root
TVD – True Vertical Depth

E – Young's Modulus, psi
K – Permeability, md
K_{IC} – Fracture Toughness, psi-inch$^{0.5}$
P_c – Closure Pressure, psi
P_i – Initial Reservoir Pressure, psi
P_o – Pore Pressure, psi
P_w – Surface Injection Pressure, psi
S_H – Maximum Horizontal Stress, psi
S_h – Minimum Horizontal Stress, psi
S_v – Vertical Stress, psi
ν – Poisson's Ratio
ν_p – compressional velocity, ft/s
ν_s – shear velocity, ft/s
ρ – density, slug/ft^3

References

1. Caicedo, H.U., Calhoun, W.M., Ewy, R.T., SPE/IADC 92576, "Unique ROP Predictor Using Bit-specific Coefficient of Sliding Friction and Mechanical Efficiency as a Function of Confined Compressive Strength Impacts Drilling Performance," presented at the SPE/IADC Drilling Conference held in Amsterdam, The Netherlands, 23-25 February 2005.
2. J.C. Rojas, D. E. Clark, J. Zhang, "Stressed Shale Drilling Strategy – Water Activity Design Improves Drilling Performance," SPE 102498, presented at the 2006 SPE Annual Technical Conference and Exhibition held in San Antonio, Texas, U.S.A., 24-27 September 2006
3. F.K. Mody and A.H. Hale, "Borehole-Stability Model To Couple the Mechanics and Chemistry of Drilling-Fluid/Shale Interactions," JPT, November 1993, pp 1093
4. Aston, M. S., Alberty, M. R., de Jong, H. J. and Armagost, K.: "Drilling Fluids for Wellbore Strengthening," SPE/IADC 87130 presented at the 2004 IADC/SPE Drilling Conference, Dallas, Texas, 2-4 March 2004.
5. Alberty, M. W. and McLean, M. R.: "A Physical Model for Stress Cages", SPE 90493 presented at 2004 SPE Annual Technical Conference and Exhibition, Houston, Texas, 26-29 September 2004.
6. Sweatman, R. E., Kessler, C.W. and Hillier, J.M.: "New Solutions to Remedy Lost Circulation, Crossflows, and Underground Blowouts," SPE/IADC 37671 presented the 1997 SPE/IADC Drilling Conference held in Amsterdam, The Netherlands, 4-6 March 1997.
7. Wang, H., Sweatman, R., Engelman, B., Deeg, W., Whitfill, D. Soliman, M. Y., and Towler, B. F.: "The Key to Successfully Applying Today's Lost Circulation Solutions," SPE 95895, presented at the 2005 SPE Annual Technical Conference and Exhibition, Dallas, Texas, 9-12 October 2005.
8. Wang, H., Towler, B.F. and Mohamed, S.Y.: "Fractured Wellbore Stress Analysis – Can Sealing Micro-cracks Really Strengthen a Wellbore?" paper SPE/IADC 104947 presented at 2007 SPE/IADC Drilling Conference, Amsterdam, The Netherlands, 20-22 February 2007.
9. Wang, H., Towler, B.F. and Mohamed, S.Y.: "Near Wellbore Stress Analysis and Wellbore Strengthening for Drilling Depleted Formations." SPE 102719 presented at the 2007 SPE Rocky Mountain Oil & Gas Technology Symposium, Denver, Colorado, U.S.A., 16–18 April 2007.
10. Wang, H., Soliman, M.Y., Towler, B. F., "Investigation of Factors for Strengthening a Wellbore by Propping Fractures," IADC/SPE 112629, presented at the 2008 IADC/SPE Drilling Conference held in Orlando, Florida, U.S.A., 4–6 March 2008.
11. Whitfill, D., Wang, H., Jamison, D. E., and Angove-Rogers, A.: "Preventing Lost Circulation Requires Planning Ahead," SPE 108647 presented at the 2007 International Oil Conference and Exhibition in Veracruz, Mexico, 27-30 June, 2007.
12. Whitfill, D., Jamison, D. E., Wang, H., and Thaemlitz, C.: "New Design Models and Materials Provide Engineered Solutions to Lost Circulation," SPE 101693 presented at the 2006 Russian Oil and Gas Technical Conference and Exhibition, Moscow, Russia, 3-6 October, 2006.
13. Wang, H., Soliman, M.Y., Whitfill, D. L., Towler, B.F., "Case Histories Show Wellbore Strengthening as a Cost-Effective Option for Drilling with Narrow Mud Weight Windows," AADE-08-DF-HO-17, presented at the 2008 AADE Fluids Conference and Exhibition held at the Wyndham Greenspoint Hotel, Houston, Texas, April 8-9, 2008.
14. Soliman, M.Y., Craig, D., Bartko, K., Rahim, Z., Ansah, J., Adams, D., "New Method for Determination of Formation Permeability, Reservoir Pressure, and Fracture Properties from a MiniFrac Test," ARMA/USRMS 05-658, presented at Alaska Rocks 2005, The 40th U.S. Symposium on Rock Mechanics (USRMS): Rock Mechanics for Energy, Mineral and Infrastructure Development in the Northern Regions, held in Anchorage, Alaska, June 25-29, 2005.

Appendix

The early development of fracture diagnostic techniques aimed at the determination of fracture closure pressure and leakoff coefficient. Later development concentrated on the transient analysis of the before-closure data leading to the calculation of reservoir properties such as initial pressure and permeability.

More recent techniques have been presented to analyze the after-closure data. These analysis techniques rely heavily on the conventional well-testing technology. One particular technique is used in this paper to determine the parametric properties of the formations being fractured during slurry injection.

After-Closure Analysis

One major weakness in some of the before-closure analysis techniques is strong dependence on an assumed fracture-propagation model. In addition the change of model dimension; fracture length and width makes a unique analysis very difficult to achieve. Analysis of after-closure data would to some extent eliminate this problem. Several models for after-closure analysis have been developed. In this paper we used a technique that we found easy to apply and which provided reliable analysis.

The technique we have used is grounded in well test analysis technology. If we consider the MiniFrac test (or a fracturing treatment for that matter) as a pump-in/shut-in test with analogy to the standard injection falloff test, we may use classical testing techniques to analyze the falloff data. Strictly speaking, the MiniFrac test is not a conventional well test because of the propagation of the fracture during the pumping period. However, the pumping period of a MiniFrac test is usually short, and specialized well-testing techniques may be applied to the falloff period with a fairly high degree of accuracy. In other words, the effect of fracture propagation during the pumping period on the fall-off period may be small enough that ignoring it will not result in significant error in the calculation.

Because the falloff period is usually much longer than the pumping period an existing well test analysis technique may be used to analyze the falloff data, beyond the closure time, for reservoir pressure and reservoir permeability. It is possible to identify one of several flow regimes depending on the reservoir, fracture and perforation schemes. These flow regimes may be linear, pseudo-radial, bilinear and spherical flow regimes. The simplest and most common is the pseudo-radial flow regime. This flow regime will be reviewed next.

Pseudo-radial Flow Regime

Equation 1 describes the behavior of the pressure data during the after-closure period when the created fracture is fairly short and the fracture has no, or little, residual conductivity. These conditions lead to pseudo radial flow condition. Equation 2 is a rewrite of equation 1 in field units. The constant 1694.4 is $\left(141.2/\left(2\times 24\right)\right)$ resulting from using time in hr and the injected volume in barrel per day. Equation 3 is the log-log form of equation 2, while equation 4 is the derivative form of equation 2. In all these equations, the time, t, is the total time of the test measured from the start of the test, meaning that it includes both the injection and shut-in times.

$$p_D = \frac{1}{2}\frac{t_{Dinj}}{t_D} \quad (1)$$

$$p_{fo}\text{-}p_i = \frac{1694.4V\mu}{kh}\frac{1}{t} \quad (2)$$

$$\log\left(p_{fo}\text{-}p_i\right) = \log\left(\frac{1694.4V\mu}{kh}\right) - \log\left(t\right) \quad (3)$$

$$\log\left(t\frac{\partial p_{fo}}{\partial t}\right) = \log\left[\frac{1694.4V\mu}{kh}\right] - \log(t) \quad (4)$$

Equation 3 indicates that if a pseudo-radial flow regime dominates the reservoir, plotting the pressure drop $\left(p_{fo}\text{-}p_i\right)$ versus total time on a log-log graph will eventually yield a straight line whose slope is -1. Equation 4 also indicates that a plot of the derivative function versus time would also yield a straight with slope of -1. The slope of the straight line of the derivative plot is only a function of observed pressure, test time and the flow regime. Thus the slope of the straight line is indicative of the pseudo-radial flow regime. Because of its independence of initial reservoir pressure and reservoir properties, it is an ideal technique to determine the prevailing flow regime.

Once the flow regime is determined to be pseudo-radial using the derivative plot, a plot of pressure versus the reciprocal of time, as per equation 2, would yield a straight line. The intercept of the straight line is the initial reservoir pressure while the slope of the straight line is a function of formation permeability. Formation permeability may also be calculated from Eqs. 2-4; however, it is recommended that equation 3 be used for that purpose.

It can be seen that the presented analysis technique is a function of the total injected volume. However it is still recommended that the injection rate is kept fairly constant during the test.

Other Flow Regimes

Three other flow regimes may be observed, linear, bilinear, and spherical. Equations 5-7 are the corresponding form of equation 1 respectively.

$$p_{fo}\text{-}p_i = 31.05\ \frac{V}{4h}\left(\frac{\mu}{\varphi c_t k L_f^2}\right)^{0.5}\left(\frac{1}{t_p+\Delta t}\right)^{0.5} \quad (5)$$

$$p_{fo}\text{-}p_i = 264.6\frac{V}{h}\left(\mu\right)^{0.75}\left(\frac{1}{\phi c_t k}\right)^{0.25}\frac{1}{\sqrt{k_f w_f}}\left(\frac{1}{t_{inj}+\Delta t}\right)^{0.75} \quad (6)$$

$$p_{fo}\text{-}p_i = 2.9434\times 10^4 V_{ch}\left(\phi c_t\right)^{0.5}\left(\frac{\mu}{k}\right)^{1.5}\left(\frac{1}{t_{inj}+\Delta t}\right)^{1.5} \quad (7)$$

The identification and analysis of the various flow regimes follows the logic discussed in the pseudo radial flow section with the exception that observed slope would be -0.5, -0.75, or -1.5 depending on the flow regime occurring in the formation. The exponent of time in the Cartesian plot will also depend on the identified flow regime. Which of these flow regimes dominates the after closure period depends on reservoir properties, fracture length, residual fracture conductivity, and the geometry of the fracture well intersection.

Tables

Table 1 Summary for Methods to Obtain the Rock Mechanical Properties and in-situ Stresses.

Critical Parameters	Methods	Possible Data Sources
Young's Modulus (E)	Calculate from shear and compressional sonic slowness and bulk density	Full waveform Sonic log, dipole Sonic log or monopole Sonic log and Bulk Density
	Ratio of stress to strain	Uni-axial core tests
Poisson's Ratio ( )	Calculate from shear and compressional sonic slowness	Full waveform Sonic log, dipole Sonic log or monopole Sonic log
	Ratio of lateral strain to longitudinal strain	Uni-axial core tests
Pore pressure (P_o)	Shale: Empirical relationship with sonic porosity or resistivity. Using NCT (Normal Compaction Trend) to infer pore pressure (Eaton's, Ratio, Equivalent depth or other empirical methods)	Seismic interpretation for interval transition velocity Sonic, density, resistivity, Dc exponent, Gamma Ray, Temperature logs
	Permeable zones: Formation Tester Measurement. Analysis on Compartmentization, fault seal, Centroid effect, Buoyancy etc.	Lithological stratigraphy for lithological horizons, faults, diapers etc. Formation testers.
	Infer from operations	Background gas, connection gas, trip gas, well kicks and mud-weight
Minimum horizontal stress (S_h)	Direct measurements	LOT, ELOT
	Stress prediction	Pore pressure, Vertical stress and Pseudo-Poisson's ratio, Empirical effective stress correlations
	Infer from operations	Water injection, hydraulic fracturing data, Mini-Frac Analysis, lost circulation data
Vertical stress (S_v)	Integrate from bulk density log	Bulk density log, Water depth, Water table depth
Maximum horizontal stress (S_H)	Sonic log interpretation; Analysis on borehole breakout related to wellbore pressure	Full waveform Sonic log Breakout image or multi-arms caliper log, wellbore pressure history
Fracture Toughness (K_{IC})	Fracture toughness lab tests	Direct test on rock or core samples

Table 2: Summary of Pressure Decline Analysis for LOT #1

LOT #1 Closure Pressure Analysis					
Method	Fluid Weight, ppg	Depth, ft	P, psi	Pc, psi	Pc, ppg
SQRT Time	9.1	7907	2755	6497	15.80
G-Function	9.1	7907	2735	6477	15.75
GdP/dG	9.1	7907	2782	6524	15.87

Table 3: Summary of Closure Pressures Based Pressure Decline Analysis

Operation	Fluid Weight, ppg	Top Perf Depth, ft	Pc_surf, psi	Pc, psi	Pc, ppg	Pc, psi/ft
LOT#1	9.1	7907	2782	6524	15.87	0.83
LOT#2	9.1	7907	3708	7450	18.12	0.94
P_Test	9.1	7623	3482	7089	17.88	0.93
Injection#1	10	7623	3337	7301	18.42	0.96
Injection#2	10.4	7623	3402	7525	18.98	0.99
Injection#3	9.2	7623	3404	7051	17.79	0.92
Injection#4	8.8	7623	3600	7088	17.88	0.93

Table 4: Formation Pressure of Claystone Formations Determined with PDA

Operation	Fluid column Weight, ppg	Top Perf Depth, ft	Pi_surf, psi	Pi, ppg	Pi, psi/ft
LOT#1	9.1	7907	720	10.85	0.56
P_Test	9.1	7623	850	11.24	0.58
Injection#1	10	7623	1490	13.76	0.72
Injection#2	10.4	7623	2768	17.38	0.90
Injection#3	9.2	7623	2630	15.83	0.82
Injection#4	8.8	7623	3223	16.93	0.88

Figures

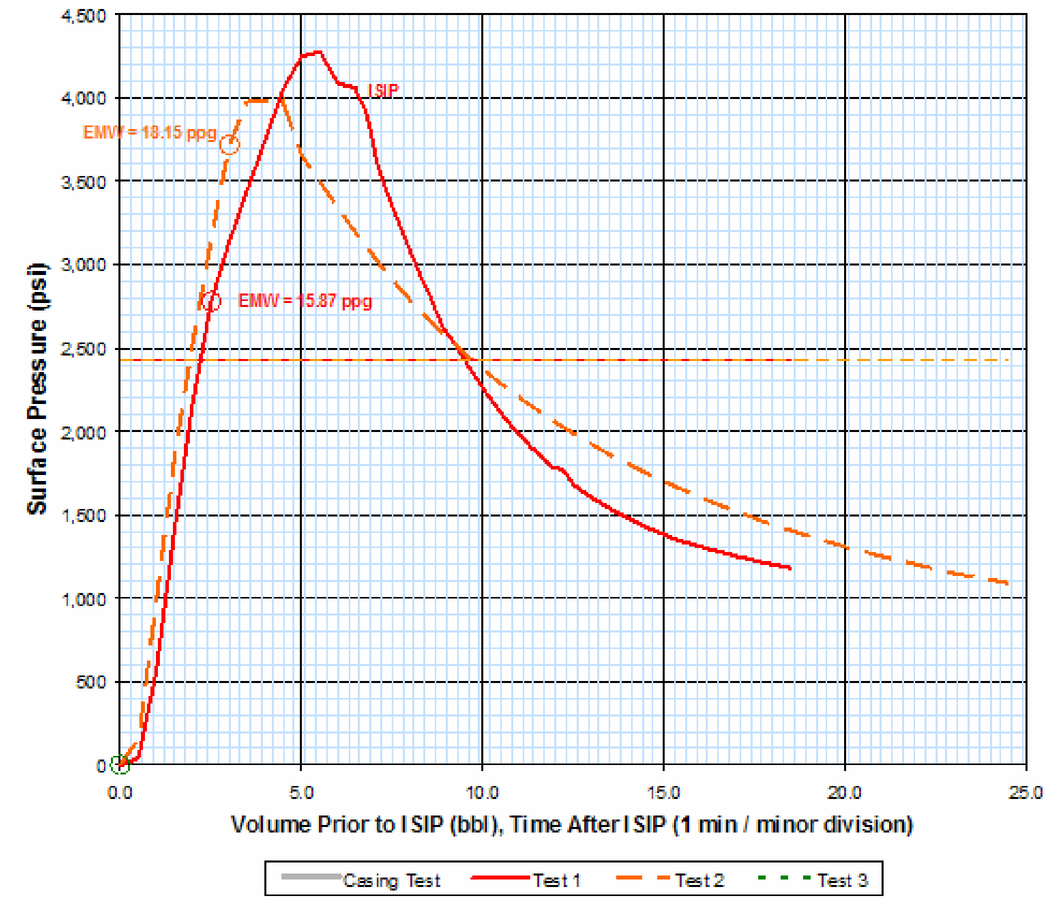

Figure 1: Results of LOT #1 and #2 for the Depth of 7907 ft

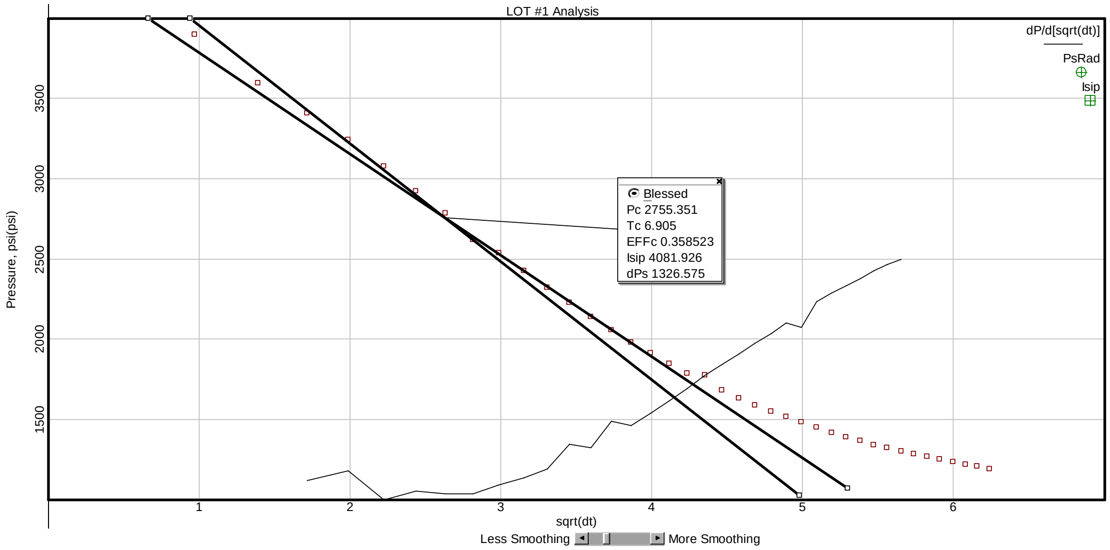

Figure 2: SQRT Time plot for LOT#1

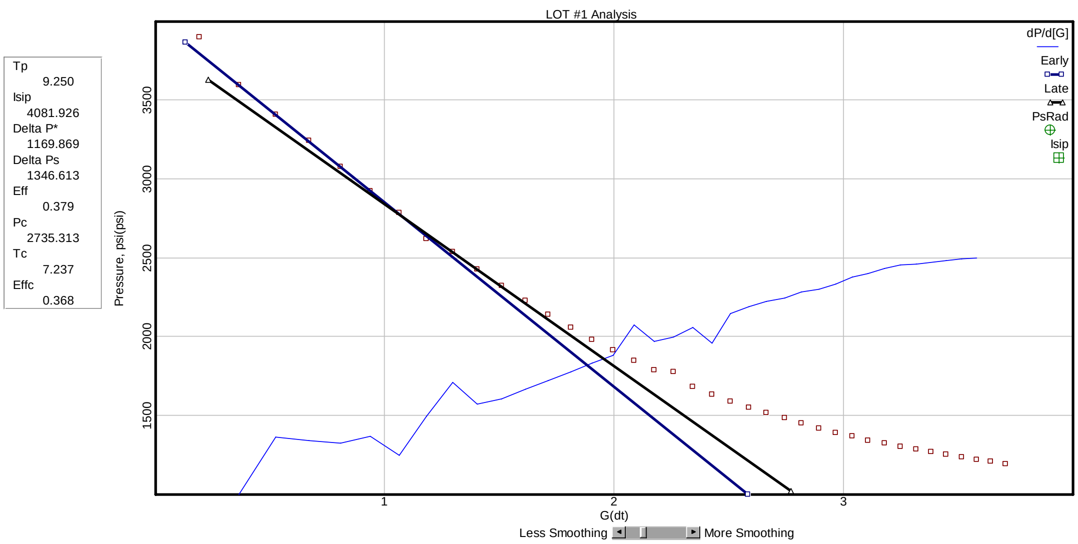

Figure 3: G-Function plot for LOT #1

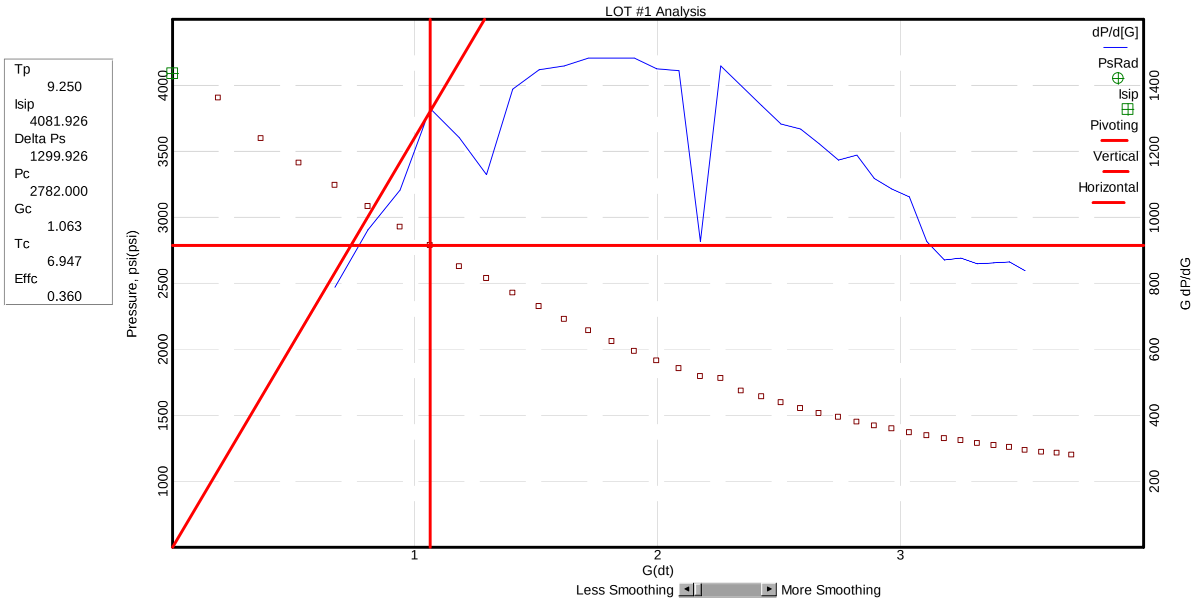

Figure 4: Gdp/dG plot for LOT #1

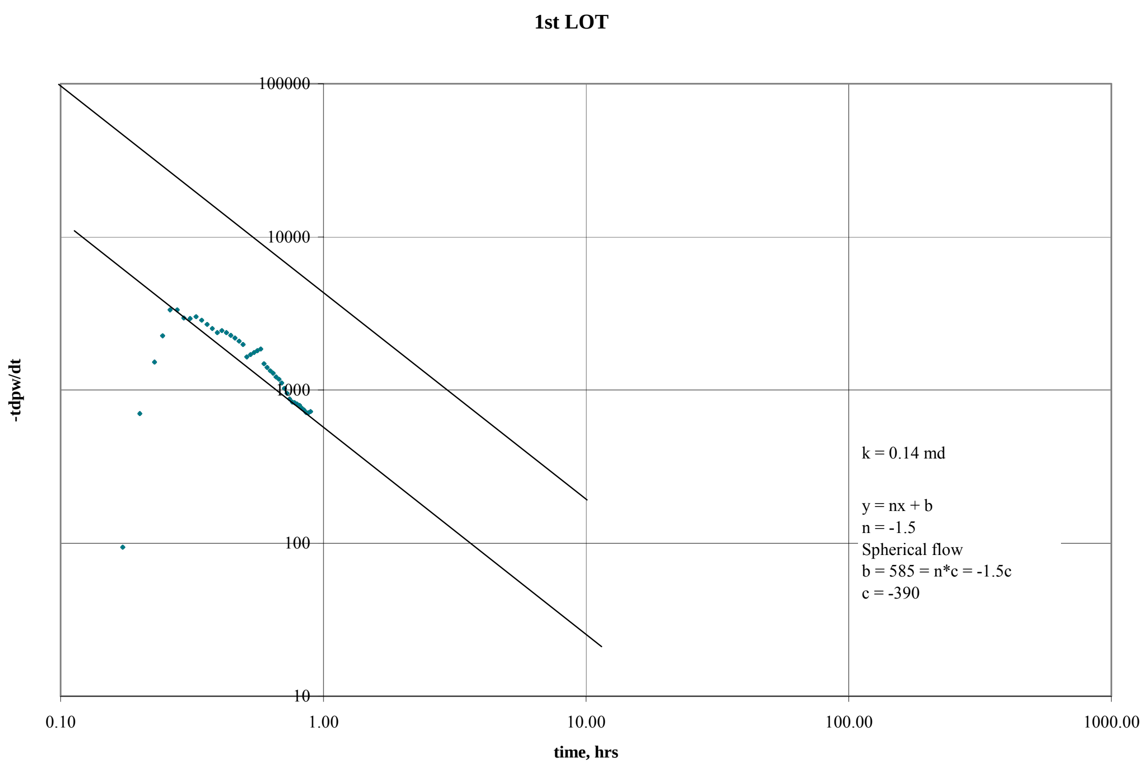

Figure 5: LOT Analysis - The slope of -1.5 indicates a Spherical Flow Regime

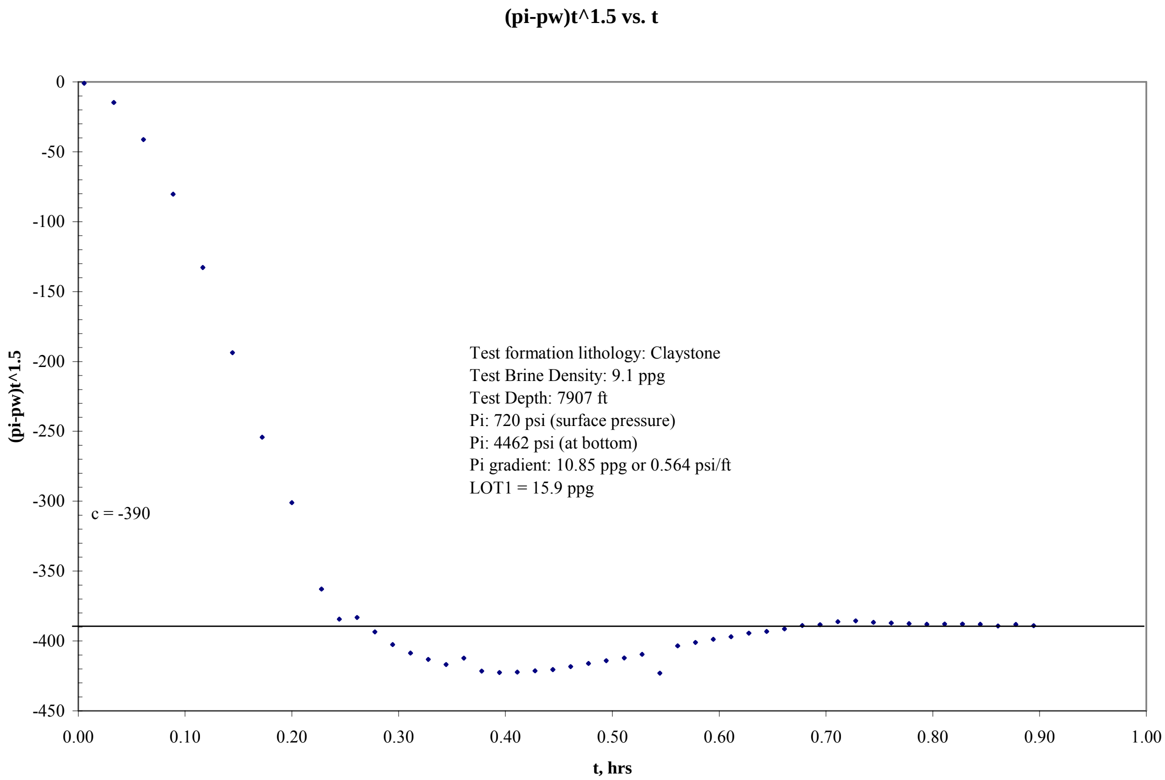

Figure 6: Permeability Calculation - K=0.14 md determined from the horizontal line of C=-390

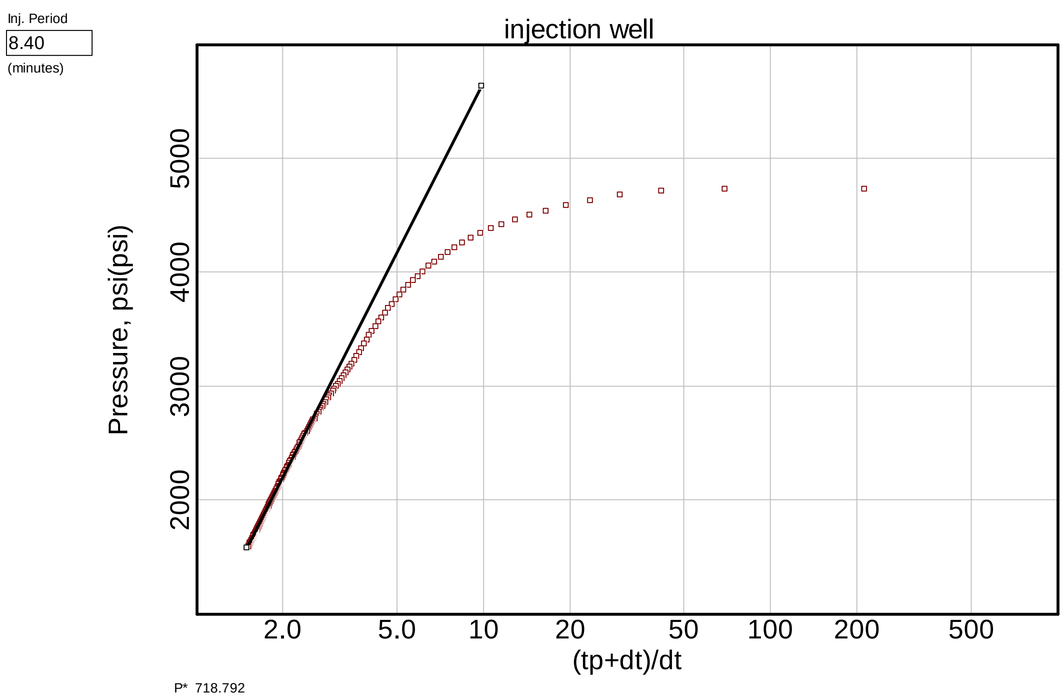

Figure 7: An Example of Horner's Plot for Formation Pressure Analysis with PDA

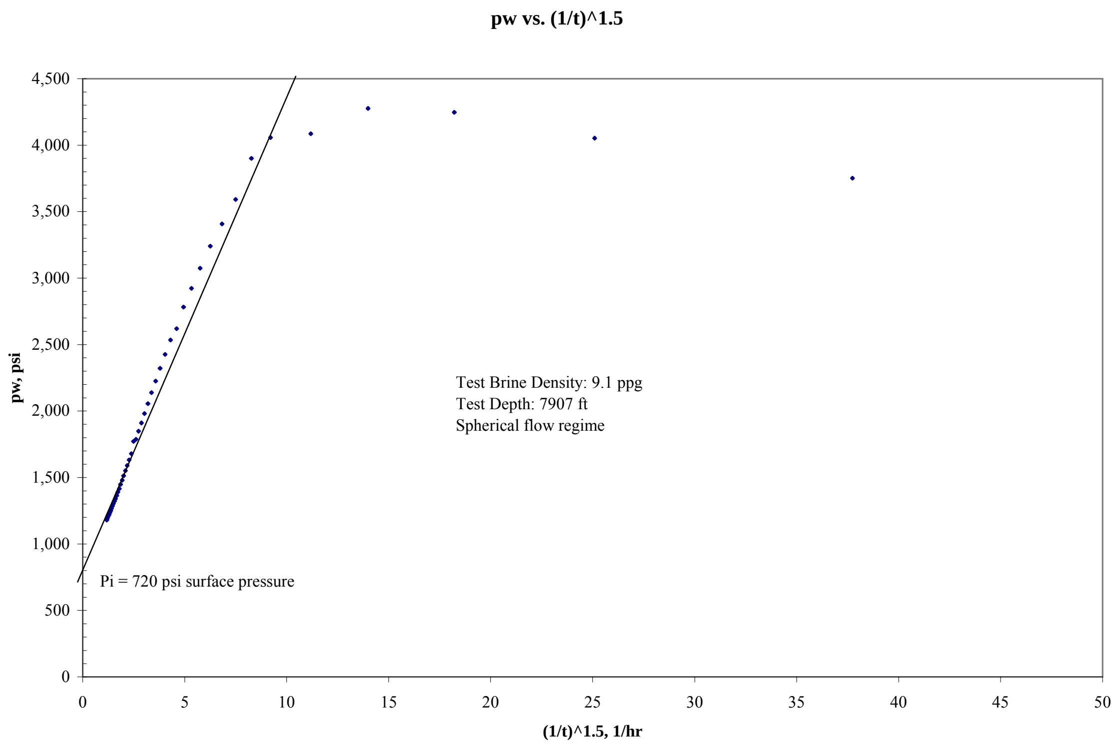

Figure 8: An Example of Soliman's Method for Formation Pressure with PDA

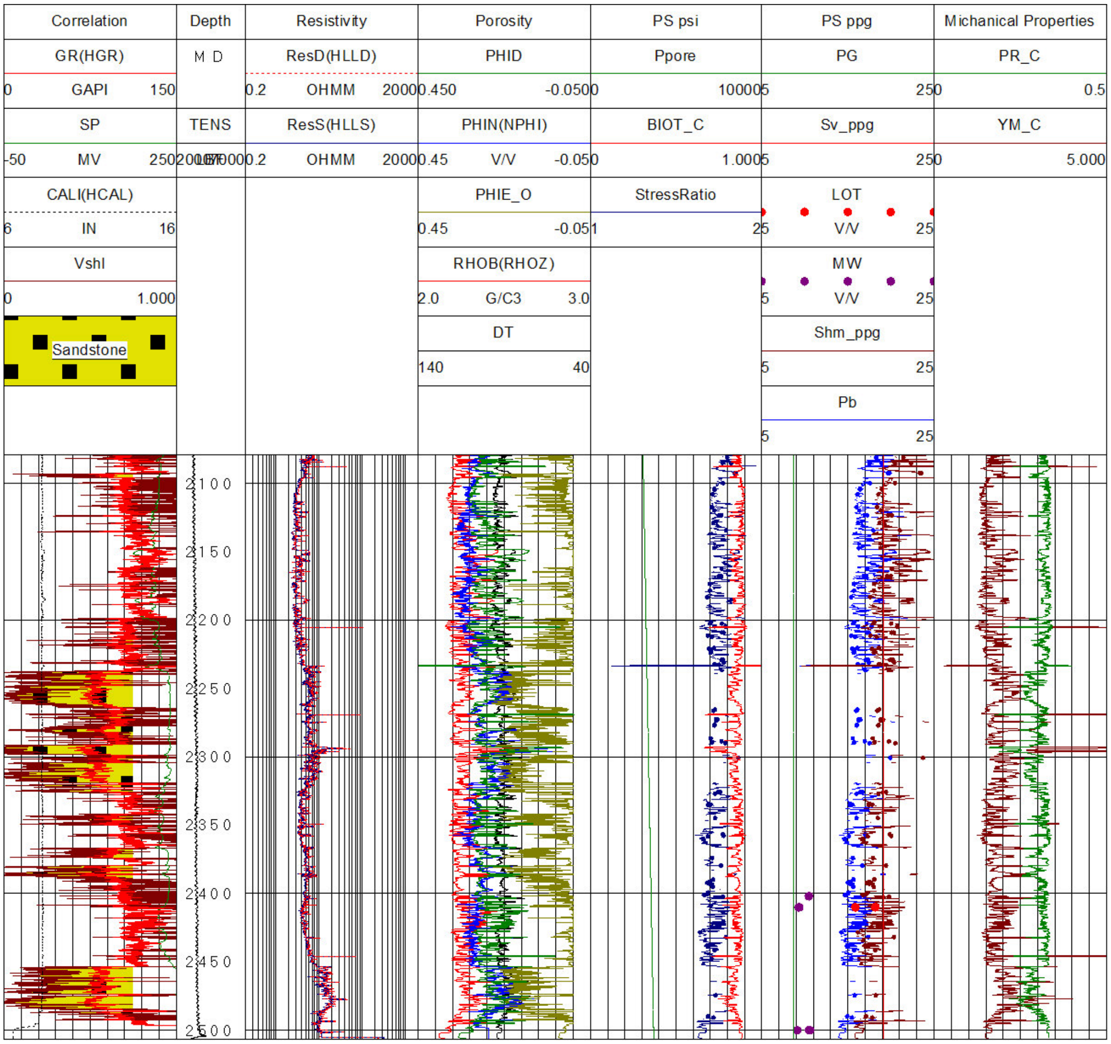

Figure 9: Log Based Analysis for Geomechanical Modeling

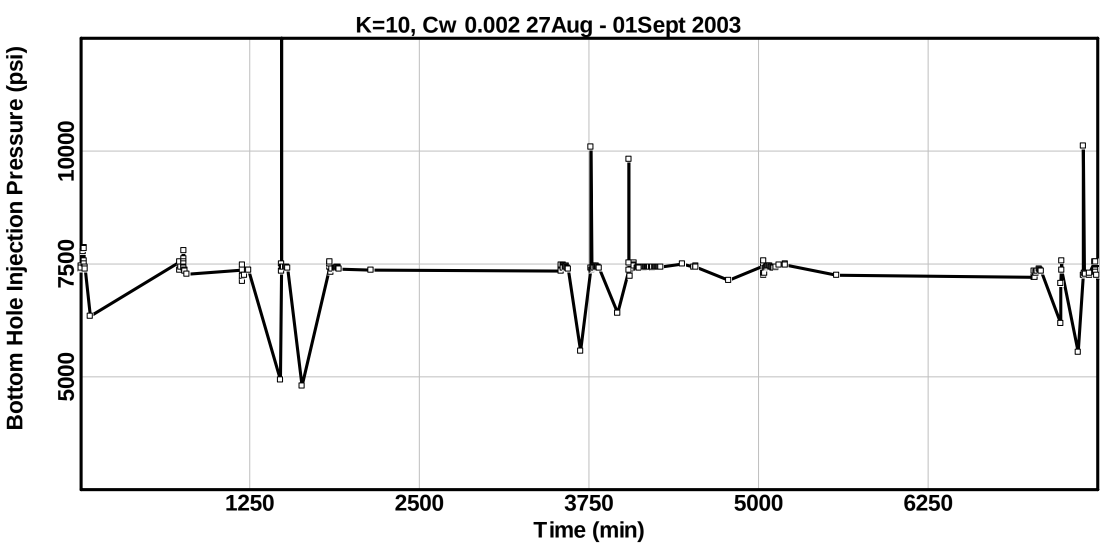

Figure 10: Simulation Results for a Multiple Batch Injection

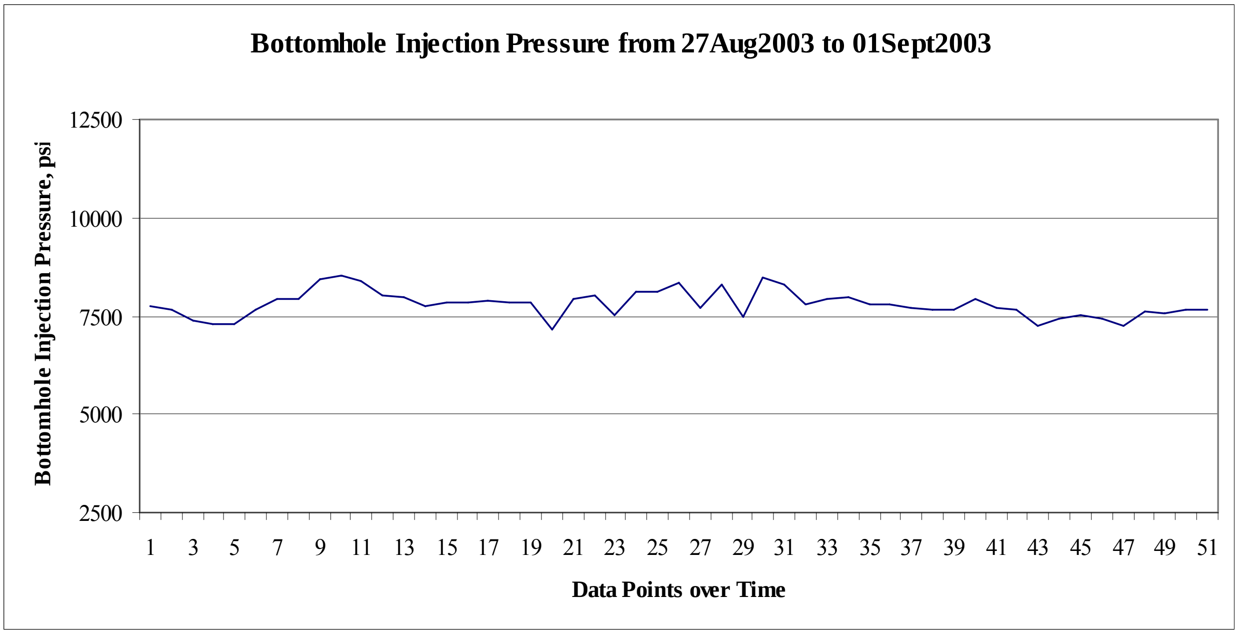

Figure 11: Recorded Pressure for a Multiple Batch Injection

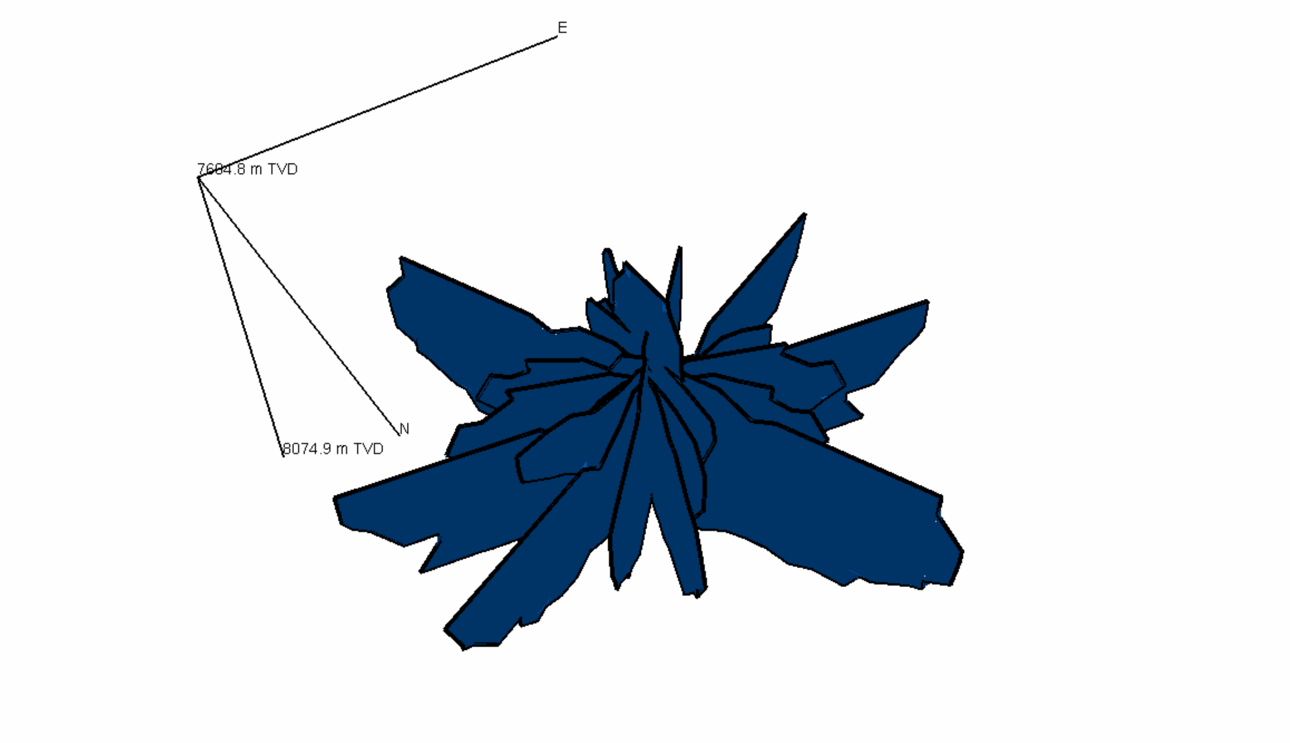

Figure 12: Simulated Multiple Fractures Created with the Injection